JGR Space Physics

RESEARCH ARTICLE
10.1029/2024JA033376

A Study on the Potential Mechanisms Underlying the Seasonal Dependence of 15MLT-PCA

Yu Wang[1], De-Sheng Han[1], Hui-Ting Feng[1], Ya-Ting Xiong[1], Hui-Xuan Qiu[1], and Yong-Liang Zhang[2]

[1]State Key Laboratory of Marine Geology, School of Ocean and Earth Science, Tongji University, Shanghai, China, [2]The Johns Hopkins University Applied Physics Laboratory, Laurel, MD, USA

Key Points:

- The reason of seasonal dependence of 15MLT-PCA was investigated by comparison of observations with global magnetohydrodynamics simulations
- Under the same interplanetary magnetic field conditions, simulations showed that the pattern of lobe reconnection is different in summer and winter
- The results indicate that the particular pattern of lobe reconnection in summer is crucial for the exclusive occurrence of 15MLT-PCA during the summer

Supporting Information:

Supporting Information may be found in the online version of this article.

Correspondence to:

D.-S. Han,
handesheng@tongji.edu.cn

Citation:

Wang, Y., Han, D.-S., Feng, H.-T., Xiong, Y.-T., Qiu, H.-X., & Zhang, Y.-L. (2025). A study on the potential mechanisms underlying the seasonal dependence of 15MLT-PCA. *Journal of Geophysical Research: Space Physics*, *130*, e2024JA033376. https://doi.org/10.1029/2024JA033376

Received 27 SEP 2024
Accepted 31 DEC 2024

Author Contributions:

Conceptualization: Yu Wang, De-Sheng Han
Data curation: Yu Wang
Formal analysis: Yu Wang, Hui-Ting Feng, Ya-Ting Xiong, Hui-Xuan Qiu
Funding acquisition: De-Sheng Han
Investigation: Yu Wang, De-Sheng Han, Ya-Ting Xiong, Hui-Xuan Qiu
Methodology: Yu Wang, De-Sheng Han
Project administration: De-Sheng Han
Resources: Yu Wang, Yong-Liang Zhang
Software: Yu Wang, Hui-Ting Feng
Supervision: De-Sheng Han
Validation: Yu Wang, Hui-Ting Feng
Visualization: Yu Wang
Writing – original draft: Yu Wang
Writing – review & editing: Yu Wang, De-Sheng Han, Hui-Ting Feng, Hui-Xuan Qiu

Abstract Specific polar cap auroras, such as 15MLT-PCA, linked to lobe reconnection due to the influence of the interplanetary magnetic field (IMF) B_y component, were only observed in the summer. Although the variance in ionospheric conductivity between winter and summer has been proposed as a potential explanation for this seasonal dependency, it has also been argued that the differences in lobe reconnection between the winter and summer hemispheres could be the cause. To address this debate, we examined two data periods with similar IMF conditions when the northern hemisphere was in summer and winter, respectively. Using DMSP/SSUSI and AMPERE observations, we detected clear 15MLT-PCA and associated field-aligned currents in the summer, but not in the winter. These observations were compared with global MHD simulations from OpenGGCM. Lobe reconnection signatures were identified for both winter and summer in the simulation results. However, a detailed analysis showed that the pattern of lobe reconnection in the winter hemisphere was different from that in the summer. Based on the combined observation and simulation results, we suggest that particular lobe reconnection in summer is critical for generating 15MLT-PCA, while the winter's reconnection may lead to transient or small-scale auroral responses that were not easily identified by DMSP/SSUSI observations as a 15MLT-PCA event.

1. Introduction

Auroras are a key phenomenon produced in the coupling processes of the solar wind, magnetosphere, and ionosphere. The primary luminous region of the aurora is known as the auroral oval, which is an oval-shaped auroral band surrounding the magnetic poles (Akasofu, 1964). The region within the auroral oval is called the polar cap, where auroras can also be frequently observed as spots or arcs (Frey et al., 2019; Hosokawa et al., 2020; Kullen, 2012). In the polar cap, it is typically empty during southward interplanetary magnetic field (IMF), but when northward, auroral spots are typically observed detached from the auroral oval, while auroral arcs are connected to the auroral oval at one or both ends.

The auroral spots in the polar cap include cusp spots (Milan et al., 2000), High-latitude dayside aurora (HiLDA) (Carter et al., 2018; Frey et al., 2003) and "space hurricane" (Zhang et al., 2021). Cusp spots and HiLDAs are typically more spot-like aurora. The cusp spots are usually bright spots in the cusp region and are believed to result from lobe reconnection when the IMF conditions are northward (Fuselier et al., 2002; Østgaard et al., 2005). It is generally believed that cusp spots are proton auroras, because they are defined based on proton auroras initially. However, Han et al. (2023) also observed cusp spots in electron auroras. The HiLDA is characterized by localized, bright far-ultraviolet (FUV) emissions observed around 15:00 magnetic local time (MLT), occurring at much higher geomagnetic latitudes than the typical cusp location (Frey et al., 2003). Frey et al. (2004) proposed that another key feature of HiLDA is its occurrence only in the summer hemisphere, under the IMF conditions positive B_z and positive B_y in the northern hemisphere, without any signature of precipitating protons in these regions. Although the HiLDAs are a typically northward IMF phenomenon (Frey et al., 2004), they may also be seen during weakly southward IMF (Cai et al., 2021). The HiLDAs have also been suggested to be generated by the lobe reconnection (Cai et al., 2021; Frey, 2007). Using auroral observations from Special Sensor Ultraviolet Spectrographic Imagers on Defense Meteorological satellites (DMSP/SSUSI), Zhang et al. (2021) noticed that a HiLDA can have spiral-arm structures, which resemble the appearance of a hurricane in a meteorological cloud image. Therefore, they named this particular phenomenon "space hurricane."

The auroral arcs in the polar cap, commonly referred to as polar cap arcs (PCAs), have been extensively studied and classified under various names based on their observed characteristics, including sun-aligned arcs (Berkey

et al., 1976), transpolar arcs (e.g., Elphinstone et al., 1991; Fear & Milan, 2012a, 2012b; Kullen et al., 2002), and a particular PCA often observed around 1500 MLT, abbreviated as 15MLT-PCA (Feng et al., 2021; Han et al., 2020).

In terms of statistical characteristics, both 15MLT-PCA and HiLDA share many similar observational properties (Frey et al., 2004; Han et al., 2020). They may be the similar auroral phenomenon and the 15MLT-PCAs are arc-like HiLDAs. Notably, both are exclusively observed in the summer hemisphere (Frey, 2007; Frey et al., 2003, 2004; Han et al., 2020). The variance in ionospheric conductivity between winter and summer has been proposed as a potential explanation for this seasonal dependence (Frey, 2007). Østgaard et al. (2018) have discussed other interpretations, for example, that the seasonal dependence is due to conductivity differences, ionospheric processes or have different sources in the magnetosphere. They suggested lobe reconnection only occurred in the summer hemisphere that is tilted toward the solar wind (Østgaard et al., 2018). Han et al. (2023) suggest that the differences of the lobe reconnection between the summer and winter hemispheres are the critical reason in determining the seasonal dependence of 15MLT-PCA. Thus, the reason for the seasonal dependence is still under debate.

To identify the key factor behind the summer-only occurrence of 15MLT-PCA, we analyzed in this study two periods of data with a steady positive IMF B_y, one in the northern hemisphere's summer and the other in its winter. In Section 2, we provide a brief overview of the data. In Sections 3 and 4, we compare these observations with global magnetohydrodynamics (MHD) simulations for the winter and summer periods, respectively. In Section 5, we discuss the most plausible explanation of the seasonal dependence of these auroral phenomena.

2. Data and Method

The Defense Meteorological Satellite Program (DMSP) operates several satellites that follow polar sun-synchronous orbits at an altitude of approximately 840 km, with an orbital period of around 101 min (Paxton et al., 1992). The Special Sensor Ultraviolet Spectrographic Imager (SSUSI) on DMSP has the capability to image the auroral oval from both hemispheres. Additionally, the study utilized data on precipitating electrons and ions detected by the Special Sensor J (SSJ) of DMSP, as well as 1-min IMF and solar wind data extracted from the OMNI data set.

We utilized AMPERE data derived from the Iridium satellite constellation. The constellation comprises over 66 satellites along with on-orbit spares, orbiting at an altitude of 780 km in polar orbits distributed across six equally spaced orbit planes. The magnetometer data were transferred from the Iridium Satellite Network Operations Center to the AMPERE Science Data Center, where they underwent processing to extract magnetic perturbation signatures associated with field-aligned currents (FACs) (Korth et al., 2010). The released data has undergone processing steps, including adjustment for satellite attitude to align with geophysical coordinates, removal of the Earth's main magnetic field, long-period de-trending, and transformation of residuals and satellite positions into Altitude Adjusted Corrected Geomagnetic (AACGM) coordinates.

The simulations of the OpenGGCM are compared with the observational results. The OpenGGCM is a sophisticated three-dimensional global magnetosphere-ionosphere model that employs nonuniform Cartesian grids to solve resistive magnetohydrodynamic (MHD) equations, incorporating current-driven instabilities. This model integrates inputs from the solar wind and IMF to calculate number densities, flow velocities, plasma pressures, and electromagnetic fields within the Earth's magnetospheric system. It accurately replicates magnetopause conditions, including the generation of reconnection and its dynamic effects, within the framework of resistive MHD theory. For further details, please consult Raeder (2003) and Raeder et al. (2008). It is important to note that the simulation results in this paper are expressed in the Geocentric Solar Ecliptic (GSE) coordinate system, wherein the x-axis extends from the Earth to the Sun, the z-axis is perpendicular to the ecliptic and points to the Earth's northern pole, and the y-axis completes the right-handed system.

3. A Data Period With Stable Positive IMF B_y in the Summer Hemisphere

3.1. Observation

Figure 1a depicts a typical example of a 15MLT-PCA event observed on 15 July 2010, in the northern hemisphere, as indicated by the red arrow. The white curve with two arrows indicates the trace of the satellite in Figure 1a. We noticed that a 15MLT-PCA was observed around 1500 MLT sector. Figure 1b shows the SSUSI

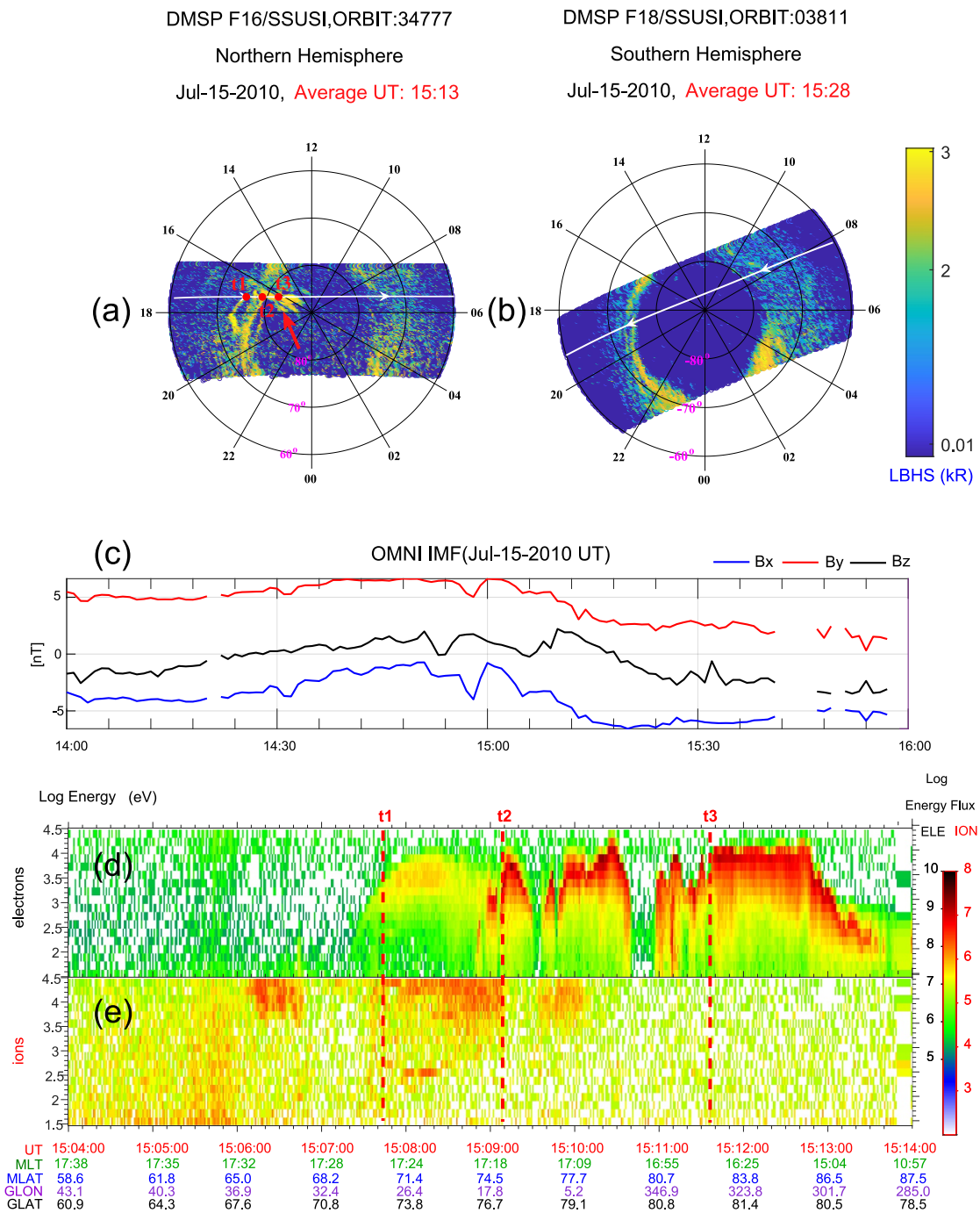

Figure 1. (a) The typical 15MLT-PCA event (indicated by the red arrow) observed on 15 July 2010. (b) The observation above the southern hemisphere during the same period. (c) The associated interplanetary magnetic field. (d)–(e) The spectrogram of differential energy flux (in units of eV/cm^2 s sr eV) for the electrons and ions respectively in the northern hemisphere.

observation in the southern hemisphere during the same time period. We see that no similar auroral structure as the 15MLT-PCA was observed in the southern hemisphere.

The panel (c) illustrates the IMF conditions from 14:00 to 16:00 UT during this day, with the blue, red, and black curves representing the B_x, B_y, and B_z components, respectively. During this period, the IMF B_y component remained positive for an extended period of time. From 14:00 to 15:10 UT, the IMF conditions remain $|B_y| >> |B_z|$ and the B_z component changed from weakly southward to weakly northward.

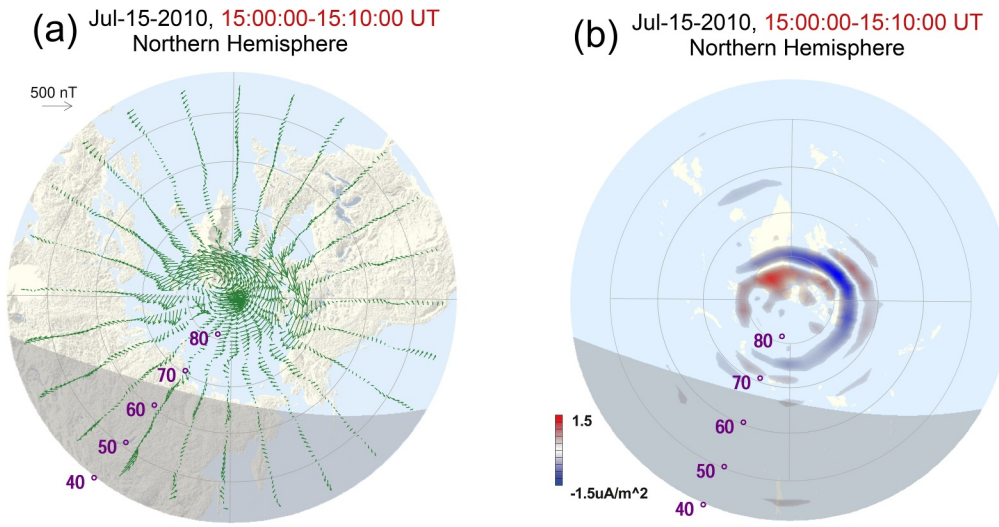

Figure 2. Spherical harmonic fit to the magnetic perturbation data and the FAC density for the northern hemisphere. The positions are translated into the AACGM system. Panel (a) shows the horizontal vector from the spherical harmonic fit evaluated with 1-hr longitude by 1° latitude resolution. Panel (b) shows the FAC density evaluated in inertial coordinates.

Panels (d) and (e) present spectrograms of the differential energy flux for electrons and ions ranging from 32 eV to 30 keV. Three red dots labeled as "t1," "t2," and "t3" on the flight path of F16 correspond to the red dotted lines labeled as "t1," "t2," and "t3" on panels (c) and (d), respectively. Between "t1" and "t2," when the satellite was traversing the auroral oval, the precipitated ions and electrons exhibited apparent properties of particles in boundary plasma sheets (Newell et al., 1991). From "t2" to "t3," as the satellite passed along the 15MLT-PCA, the electron spectrogram also displayed a monoenergetic inverted-V structure, suggesting quasi-static electron acceleration (Frey, 2007; Newell, 2000). These observations of particle precipitation properties are consistent with previous studies (Feng et al., 2021; Han et al., 2020).

Also, we examined the magnetic field disturbances and current distribution during the period from 15:00 to 15:10 UT on 15 July 2010, using magnetic field data provided by AMPERE. Figure 2 presents a ten-minute snapshot of the data along with the corresponding spherical harmonic fit and FACs derived as the curl of the spherical harmonic magnetic perturbation fit. Figure 2a covers the northern hemisphere region from 40° magnetic latitude (MLAT) to the magnetic pole. It depicts the horizontal vector from the spherical harmonic fit evaluated with a resolution of 1 hr longitude by 1° latitude in the northern hemisphere. In Figure 2a, a significant disturbance in the horizontal vector is evident from 70° MLAT to the pole in the northern hemisphere, propagating counterclockwise, with the vortex center approximately at ∼15:00 MLT and ∼85° MLAT.

Figure 2b shows the FAC density evaluated in inertial coordinates in the northern hemisphere. Upward currents are depicted in red, and downward currents in blue. Current densities with magnitudes below 0.2 m-A/m^2 are omitted due to being below the noise level in the processed data. The cell shape manifests as rounded in the dusk side and crescent in the dawn side. The FAC pattern indicates that it is consistent with ionospheric convection for $B_y > 0$ (Milan & Grocott, 2021). In the ∼1500 MLT sector, there is a strong upward FAC, that is, there is a large amount of electron precipitation.

3.2. Simulation

In this study, we employed the Community Coordinated Modeling Center (CCMC) to automatically generate 1-min OMNI data for input, and we conducted simulations using the OpenGGCM to analyze the 15MLT-PCA event from 14:00 to 16:00 UT on 15 July 2010. The magnetospheric grid spans from 20 R_E sunward of the Earth to X = −100 Re tailward, and from −50 R_E to 50 R_E in the lateral Y directions, while the ionospheric grid extends from −0.643 R_E to 0.643 R_E in the lateral X and Y directions. These simulations provided valuable insights into the behavior of the magnetosphere and ionosphere associated with the 15MLT-PCA.

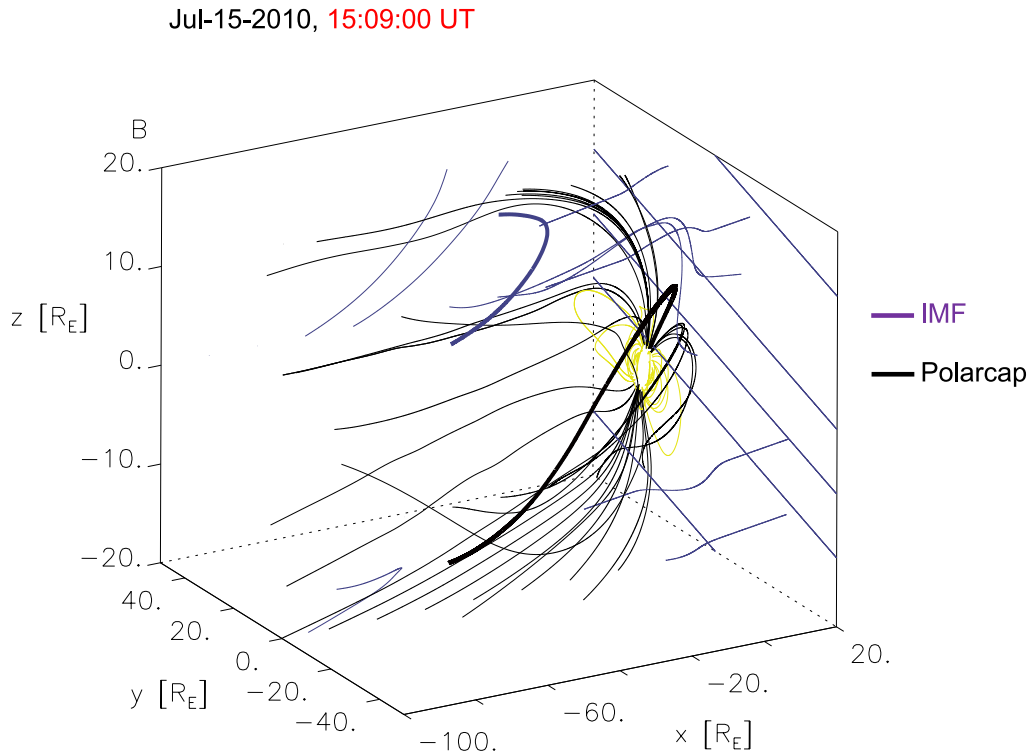

Figure 3. The flowlines from 3D perspective based on the simulation of OpenGGCM.

Figure 3 depicts the 3-D flowlines illustrating high-latitude magnetopause reconnection between the IMF and the geomagnetic field. In Figure 3, the IMF is denoted by blue lines, the open field lines are presented in black, and the closed field lines in yellow. To enhance clarity regarding the magnetic field lines post-lobe reconnection, we opted to conceal irrelevant and cluttered field lines while accentuating the reconnected field lines. This approach enables a clearer visualization of the lobe reconnection process. The 3-D flowlines distinctly reveal lobe reconnection occurring on the duskside of the northern hemisphere.

To ensure the reliability of lobe reconnection occurrence in northern hemisphere, we analyzed the magnetospheric profile at different times during the data period in both hemispheres. Here we choose an adjacent time interval of 10 min. As shown in Figure 4, bolded field lines represent those involved in the reconnection process, akin to the 3-D flowlines in Figure 3. In Figures 4a–4d, the IMF (depicted by blue field lines) undergoes reconnection with the tailward semi-open lobe field lines (green), resulting in the formation of bent green semi-open field lines connected from the Earth to the magnetosphere, along with blue free field lines post-reconnection. The green lines have draped poleward, and the blue lines appear curved in an arrow-like fashion. This configuration is indicative of the described reconnection scenario, supporting the hypothesis that the generation of 15MLT-PCA is driven by lobe reconnection. Notably, in the northern hemisphere, the formation of bent green and blue field lines occurs predominantly on the dusk side of the high-latitude magnetopause. This phenomenon is attributed to a substantial IMF clock angle, leading to an increased magnetic shear angle (where the IMF is nearly anti-parallel to the geomagnetic field) on the dusk side (Trattner et al., 2021). For northward IMF with nonzero B_y, high-latitude lobe reconnection is expected. On the whole, Figures 4a–4d illustrate that the magnetic field line topology following lobe reconnection in the northern hemisphere remains largely consistent. For the 15MLT-PCA in the summer hemisphere, the particular lobe reconnection signature is very easy to find and the reconnection shows long duration. In order to show the particular continuous signatures of magnetic field lines draping poleward very well in the summer hemisphere, we provide the simulation results for summer in Supporting Information S1. However, on the opposite hemisphere, we do not observe the presence of magnetic field lines with similar topology, whether on the dawnside or the duskside, as shown in Figures 4e–4h. This implies that when lobe reconnection occurs in the summer hemisphere, it does not happen simultaneously in the winter hemisphere.

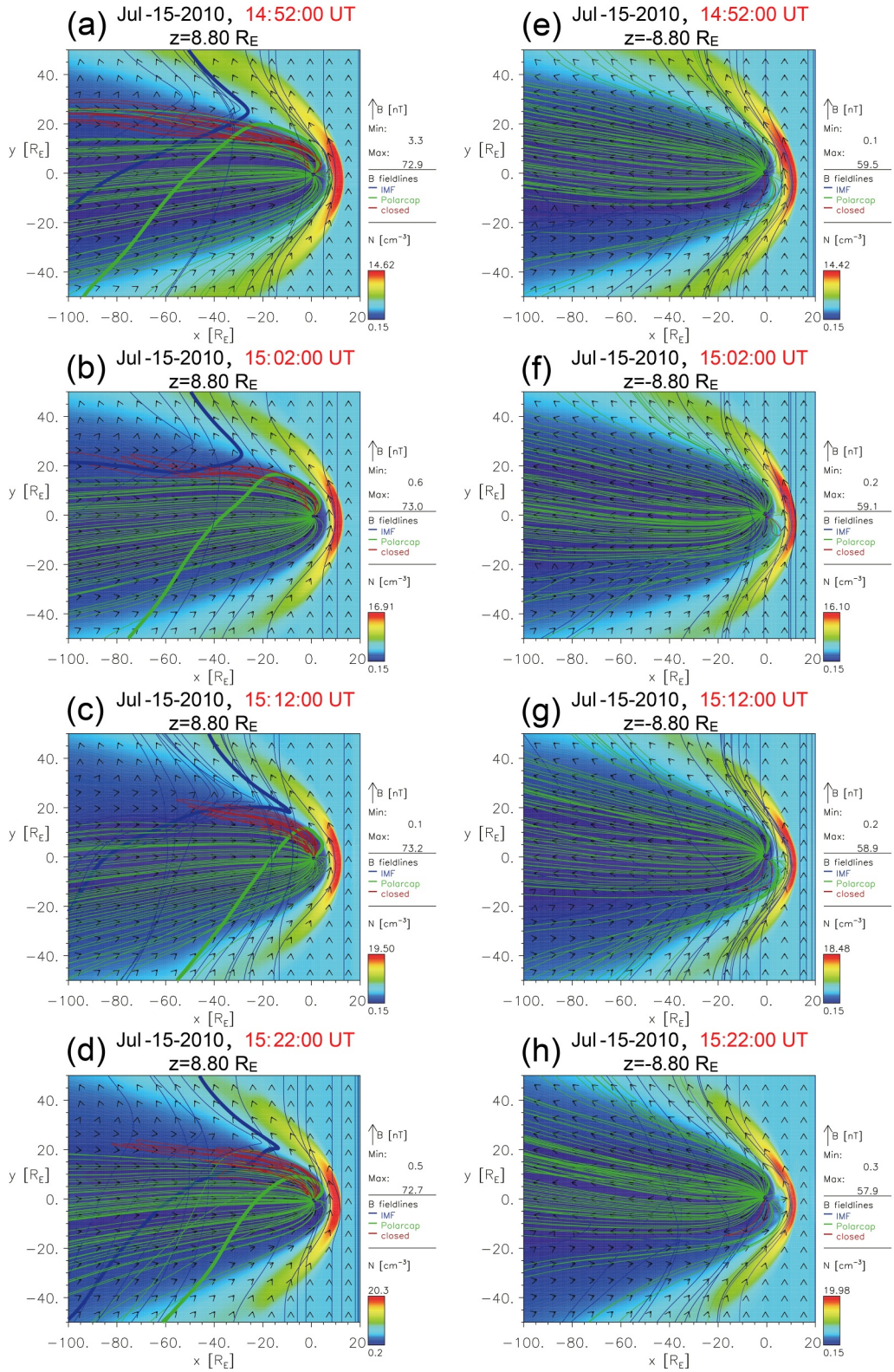

Figure 4. The magnetospheric profiles of simulation results. (a–d) The simulation results of the 15MLT-PCA event on 15 July 2010, at 14:52:00 UT, 15:02:00 UT, 15:12:00 UT, and 15:22:00 UT in the XY plane at $z = 8.8$ R_E, respectively. (e–h) The simulation results at the same time in the XY plane at $z = -8.8$ R_E. The semi-open lobe field lines are depicted by green field lines, and the free field lines are depicted by blue field lines.

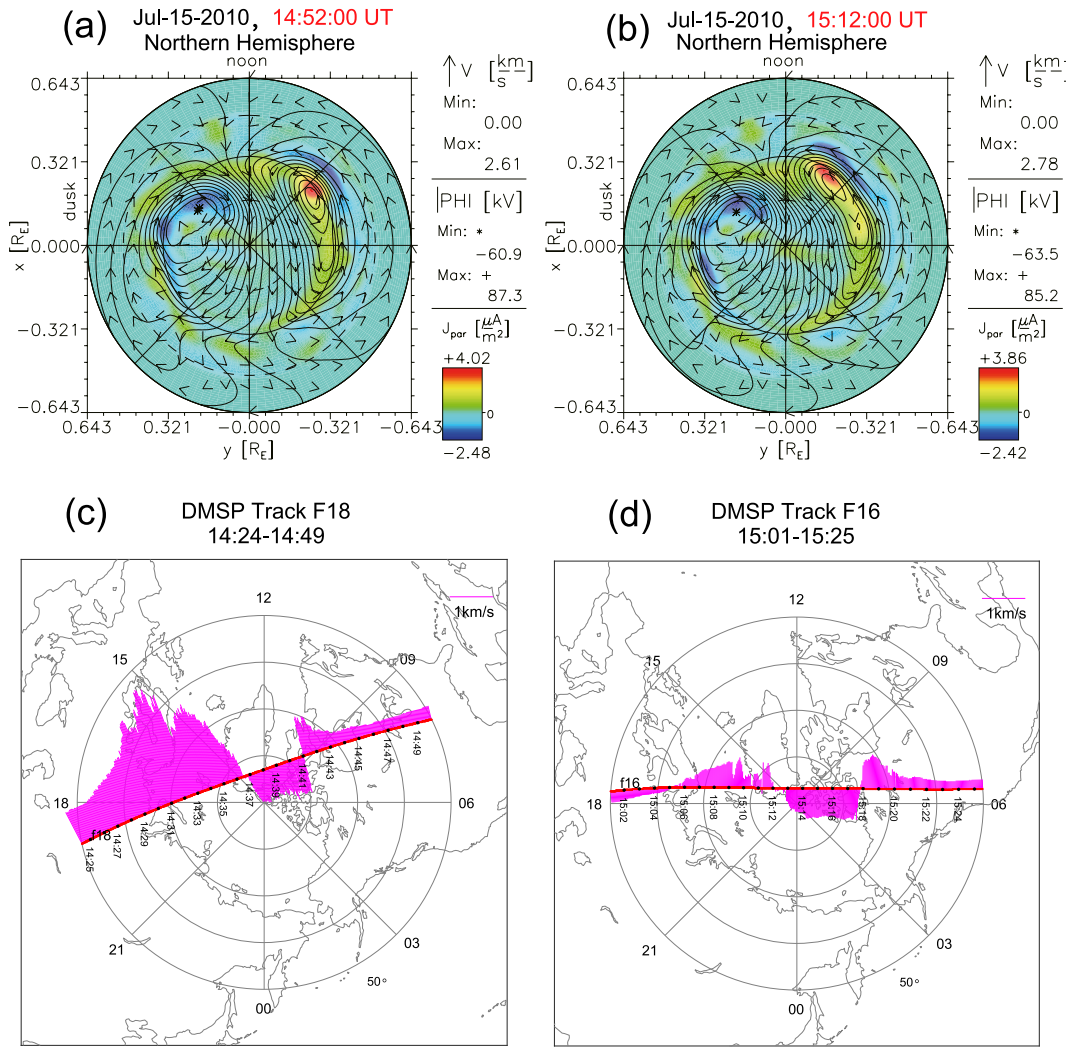

Figure 5. Panels (a) and (b) are the simulation results of 2-D ionosphere electrodynamics for northern hemisphere. Panels (c) and (d) are the convection velocities of the DMSP satellite at each location on the track.

The convection is visualized through streamlines representing the flow, which, as will be demonstrated, also serve as contours of electrostatic potential. Primarily, the convection patterns depicted in Figures 5a and 5b exhibit a twin-cell configuration with anti-sunward flow across the polar cap and sunward flow at lower latitudes, whose intensity is contingent upon the north-south component of the IMF B_z (Milan & Grocott, 2021). This pattern can be comprehended within the framework of the open model of the magnetosphere proposed by Dungey (1961). In the northern hemisphere, the reversal of convection cell shape manifests as rounded in the duskside and crescent in the dawnside. In the dusk sector around ∼1500 MLT, a greater flow shear results in increased upward FAC and more intense auroral precipitation. In the same hemisphere, there was minimal variation between the two convection patterns observed 20 min apart, indicating the stability of convection. This stability suggests that auroral phenomena should also remain stable, akin to the typical behavior observed with 15MLT-PCA, which often persists for tens of minutes up to hours (Cai et al., 2021; Feng et al., 2021; Han et al., 2020). Panels (c) and (d) show the convective velocity of the DMSP satellites at each position on the track during the corresponding time period. By comparing the simulations with the observations, they are very consistent.

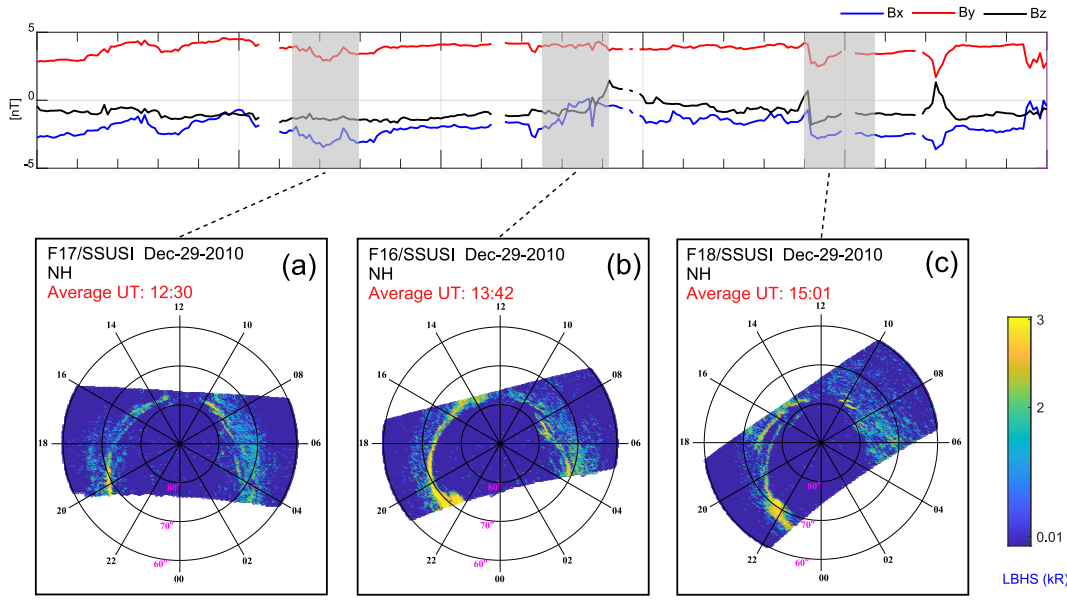

Figure 6. The panels (a–c) in the bottom are the observations by SSUSI/DMSP on 29 December 2010. The above is IMF conditions in GSE coordinate, where the blue, black, and red curves are the IMF B_x, B_y, and B_z, respectively. The gray shaded rectangles correspond to the recording time of the SSUSI images (a–c).

4. A Data Period With Stable Positive IMF B_y in the Winter Hemisphere

4.1. Observation

Figure 6 shows a period with stable positive IMF B_y on 29 December 2010, which was observed in the northern hemisphere. The upper panel is IMF conditions from 11:00 UT to 16:00 UT, with the blue, red, and black curves are B_x, B_y, and B_z components, respectively. During this period, the IMF B_y component remained positive for an extended period of time. The IMF conditions remain $|B_y| >> |B_z|$ and most of the time B_z component remained negative. Figures 6a–6c are auroral spectrum images in LBHS observed by DMSP/SSUSI. In contrast to the results shown in Figure 1a, no 15MLT-PCA occurred in this case. Long-term observations from DMSP/SSUSI corroborate the absence of a similar auroral structure as the 15MLT-PCA in winter and the auroral oval boundary appears smooth in the ∼1500 MLT sector.

We also used the data provided by AMPERE to examine the magnetic field disturbance and current distribution during the period of 12:20 to 12:30 UT on 29 December 2010. The layout of Figure 7 is the same as Figure 2. Figure 7a shows almost no magnetic field disturbance associated with lobe reconnection in winter. Figure 7b shows that FACs are concentrated on the dawn and night side, with FAC density much lower than that in summer. In ∼1500 MLT sector, there is a very weak FAC.

4.2. Simulation

Using the OpenGGCM with 1-min OMNI data as input, we further simulated the data period from 11:00 to 16:00 UT on 29 December 2010. We set the grid spans of the simulation results to be consistent with the simulation results of the previous data period in the summer hemisphere. In this data period, the magnetic field lines with the features of lobe reconnection are still very rich, that is, lobe reconnection occurs frequently in winter. However, after lobe reconnection, the magnetic field lines draping toward dawn are rarely present.

The simulation results of the 15MLT-PCA event on 15 July 2010, at 14:52:00 UT, 15:02:00 UT, 15:12:00 UT, and 15:22:00 UT in the XY plane at z = 8.8 RE, respectively.

In Figure 8, we analyzed the magnetospheric profile in the XY plane at z = 8.8 R_E. The magnetic field lines involved in the lobe reconnection process have been bolded. The green bolded line connects from the Earth to the magnetosphere and drapes poleward. The blue bolded line is free and appears curved arrow-like. The topological changes in these lines showed in Figures 8a and 8d indicate the occurrence of lobe reconnection. In Figures 8b and

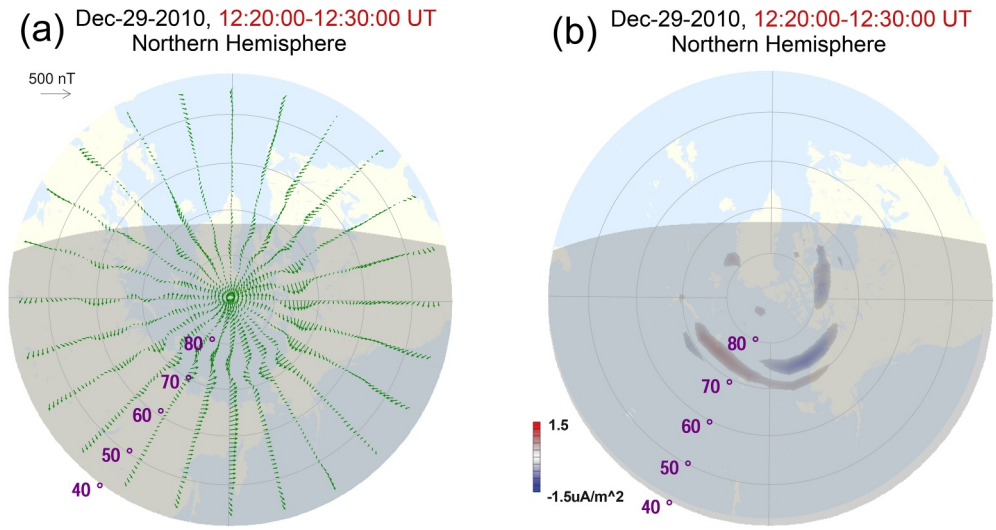

Figure 7. Spherical harmonic fit to the magnetic perturbation data and the FAC density from 12:20:00–12:30:00 UT, on 29 December 2010. Panel (a) shows the horizontal vector from the spherical harmonic fit evaluated with 1-hr longitude by 1° latitude resolution. Panel (b) shows the FAC density evaluated in inertial coordinates.

8c, we cannot see similar topological features of magnetic field lines. The magnetic field lines draping poleward are very rare, existing only at a few moments during this data period. In order to present the pattern of lobe reconnection very well in the winter hemisphere, we provide the simulation results for winter in Supporting Information S1.

Figure 9 shows the 2-D ionosphere electrodynamics on 11:48 UT and 12:28 UT, respectively. The convection patterns also exhibit a twin-cell configuration and assume a half-moon shape, with the twin cell being delimited by the 09:00 MLT–21:00 MLT line. The overall flow on the left side is clockwise, and the flow on the right side is counterclockwise. The FACs and Pedersen current are weak in intensity. In ∼15:00 MLT sector, there is no enhancive upward FACs near the convective vortices.

5. Discussion

The 15MLT-PCA and HiLDA have been exclusively observed in the summer hemisphere (Frey, 2007; Han et al., 2020). The reasons for the seasonal dependence of 15MLT-PCA and HiLDA should be the same. What is the reason for this seasonal dependence is still controversial. In this study, we present observational and simulation results for two data periods with similar IMF conditions, corresponding to the northern hemisphere's summer and winter, respectively. The DMSP and AMPERE observations indicated a significant 15MLT-PCA and associated FACs in summer, but not in winter. The simulation results indicated different patterns of lobe reconnection between winter and summer. In the winter hemisphere, the magnetic field lines draping poleward appear to be much rarer than in the summer hemisphere. We believe that the magnetic field lines draping poleward after lobe reconnection are the key to the generation of 15MLT-PCA. Considering the following reasons, we propose that the different lobe reconnection patterns between the summer and winter hemispheres are the critical factor determining the exclusive occurrence of the 15MLT-PCA in the summer hemisphere.

5.1. The Challenge of Ionospheric Conductivity in Explaining the Seasonal Dependence of 15MLT-PCA and HiLDA

Previous study has suggested that the enhanced ionospheric conductivity in summer could be the potential explanation for this seasonal dependence. The two key ionospheric and magnetospheric properties that differ between summer and winter are the ionospheric conductivity and the dipole tilt angle. The largest positive dipole tilt angle occurs during the northern summer, and the change of the dipole tilt leads to variations in distributions of ionospheric potential and FACs (Papitashvili et al., 1994). Frey (2007) suggested that solar extreme ultra-violet (EUV) illumination of the polar cap in the summer hemisphere enhances ionospheric conductivity, allowing the

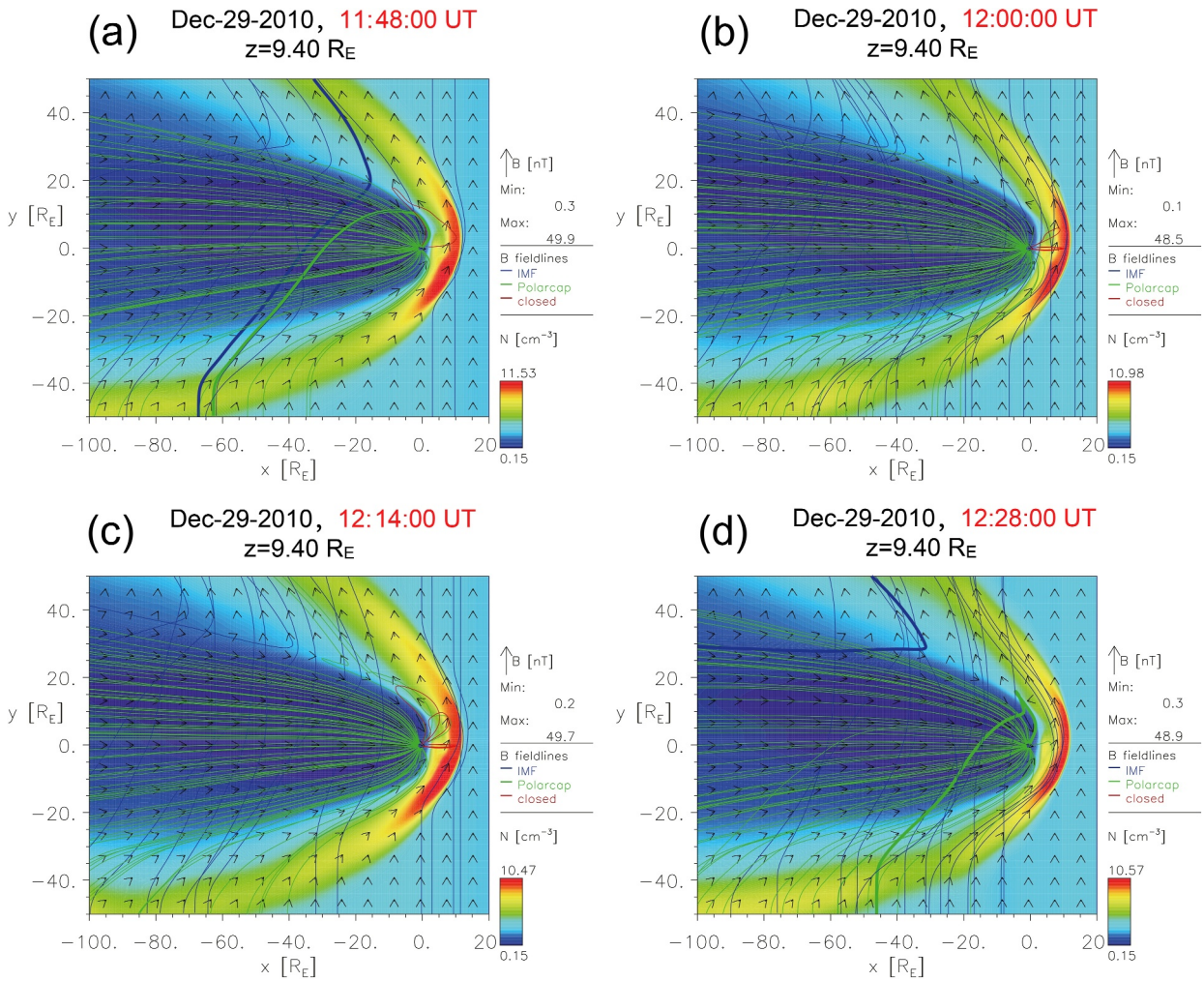

Figure 8. The magnetospheric profiles of simulation results on 29 December 2010, at 11:48:00 UT, 12:00:00 UT, 12:14:00 UT, and 12:28:00 UT in the XY plane at $z = 9.4$ R_E, respectively.

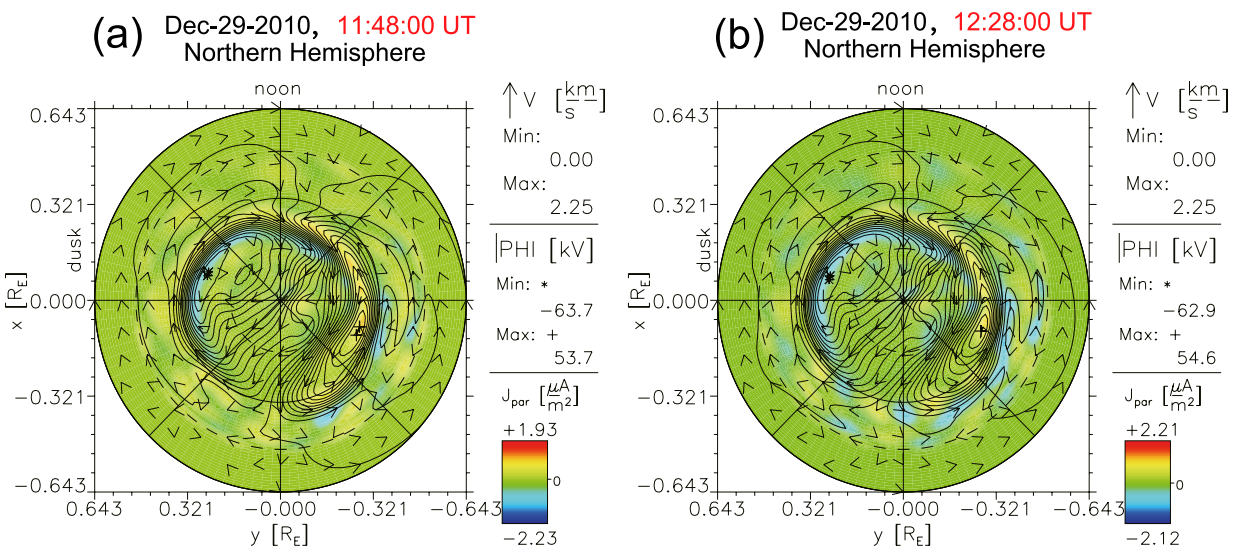

Figure 9. The simulation results of 2-D ionosphere electrodynamics for northern hemisphere.

downward current in the cusp to connect with the upward current poleward. Consequently, this process results in larger FACs during the summer than in the winter, which accounts for the seasonal dependence of HiLDA.

Among all the polar cap auroras, the cusp spot, HiLDA/'space hurricane, and 15MLT-PCA are observed in the dayside sector and are all attributed to lobe reconnection. Cai et al. (2021) showed that the origin of HiLDA should be the lobe just tailward of the cusp. Further, Cai et al. (2021) have been discussed the different HiLDA forms in detail and connected them to slightly different IMF conditions. Han et al. (2023) pointed out that their differently-appearing auroral forms observed in the dayside polar cap just reflect the different reconnection sites influenced by different IMF B_y. If the ionospheric conductivity plays a crucial role in generating the seasonal dependence of 15MLT-PCA and HiLDA, the cusp spot should be equally as rare as 15MLT-PCA and HiLDA in the winter. However, Han et al. (2023) revealed that the cusp spot can be frequently observed in the winter. This poses a challenge to the explanation for the seasonal dependence by the ionospheric conductivity.

Therefore, the explanation that ionospheric conductivity leads to the seasonal dependence of HiLDA and 15MLT-PCA is questionable.

5.2. The Lobe Reconnection and Seasonal Dependence of 15MLT-PCA

The magnetic field reconnection plays a pivotal role in the solar wind-magnetosphere coupling. For a purely northward IMF, it has been suggested that the magnetic reconnection occurs in the cusp (Fuselier et al., 2002). In reality, a purely northward IMF condition is exceptionally rare, and the typical IMF vector includes non-zero components in the *Y*-direction. Crooker (1979) and Luhmann et al. (1984) investigated the effects of a non-zero IMF B_y component during northward IMF conditions on the location of anti-parallel magnetic reconnection at the magnetopause. According to their model scenarios, magnetic reconnection does not occur at the standoff location near the subsolar magnetopause, where the magnetic fields in the two regions are not anti-parallel. The anti-parallel merging theory (Reiff & Burch, 1985) predicts that the reconnection site occurs in regions with the highest magnetic shear at the magnetopause. With a northward IMF and a large positive IMF B_y component, the reconnection site shifts to the dusk sector in the northern hemisphere. As the magnitude of northward IMF conditions intensify, these reconnection sites move to higher latitudes and farther behind the Earth (Liou & Mitchell, 2019; Trattner et al., 2021). Zhu et al. (2015) investigated the dipole tilt angle effect on magnetic reconnection locations on the magnetopause, which has a controlling effect of the dipole tilt angle to the reconnection sites.

As presented in Figure 1c, from 15:00 UT to 15:10 UT, the IMF conditions was B_y-component take predominantly with $B_z > 0$. The IMF conditions mentioned above are exactly the favorable IMF for the occurrence of 15MLT-PCA (Feng et al., 2021; Han et al., 2020). Thus, under the IMF conditions shown in Figure 1c, simulation results at different times in Figures 4a–4d all show the occurrence of lobe reconnection on the northern hemisphere's dusk side. As shown in Figure 2a, the vortex center of a magnetic disturbance at high latitudes is the footprint in ionosphere where the lobe reconnection occurs in magnetosphere, which is also the region where the 15MLT-PCA was observed. The particle precipitation properties also showed lobe reconnection characteristics (Feng et al., 2021; Han et al., 2020). Therefore, we suggest that lobe reconnection is closely related to the creation of 15MLT-PCA, and lobe reconnection provides the source driving force for it.

Considering the structure of 15MLT-PCA, we suggest it is the result of the dragging motion of the reconnected polar cap magnetic field lines caused by magnetic tension and the ionospheric convection driven by it. As depicted in Figures 4a–4d, the magnetic tension force exerted on a newly opened field line on the dayside now has a substantial Y-component, pulling it toward dawn or dusk depending on the sign of IMF B_y. For a positive IMF B_y, this results in the transfer of magnetic flux from the dayside dusk reconnection site in the northern hemisphere toward the high-latitude lobe on the dawnside.

It is widely accepted that reconnection sites, when combined with solar wind drag, contribute to ionospheric plasma convection (Ruohoniemi & Greenwald, 1996), FACs (Burch et al., 1985; Weimer, 2001), and potentially dayside auroras (Murphree et al., 1981). Postnoon auroras coincide with the presence of upward region-1 FACs (Iijima & Potemra, 1976). Auroral arcs on the dayside are associated with heightened upward FACs and a significant convection reversal in the ionosphere. Plasma convection within the ionosphere can generate FACs that are proportional to flow vorticity (Sato & Iijima, 1979). Under northward IMF conditions with a strong positive B_y and negative B_x, high-latitude reconnection drives downward FACs and more intense auroral precipitation,

consistent with observations in Figure 1d. Ionospheric convection intensifies, and the strong positive B_y induces nearly a 90° rotation of the typical two-cell convection pattern, with morning and afternoon cells (Le et al., 2002). This convection model may elucidate the expansion of postnoon auroras to higher latitudes during positive IMF B_y. Positive IMF B_y can lead to the expansion of the larger dusk cell to higher latitudes, along with its associated FACs, as depicted in Figures 2b, 5a, and 5b. Electron precipitation linked to these currents can generate auroras at higher latitudes, potentially explaining the structure of the 15MLT-PCA.

For the seasonal dependence of the 15MLT-PCA, we suggest that the different lobe reconnection patterns between the summer and winter hemispheres play a critical role. The occurrence probability of lobe reconnection is considerably lower in winter, especially when the IMF B_y component is dominant (Gou et al., 2016; Reistad et al., 2021). Han et al. (2023) predicted that lobe reconnection is difficult in the winter hemisphere when the IMF B_y is dominant. Gou et al. (2016) suggested that the asymmetry distribution of solar wind entry events in the northern and southern lobes could be caused by the variation of magnetic dipole tilt. Han et al. (2020) suggested that the effect of the tilt angle on the occurrence of 15MLT-PCA may lie in that the solar wind magnetic energy flux can be more efficiently accumulated on the tail lobe with a large tilt angle, while the solar wind magnetic energy flux determines the amount of energy that enters the magnetosphere (Akasofu, 1980). In this study, we found that lobe reconnection in winter can occur as frequently as it does in summer, as shown in Figures 4a–4d and 8. Due to the dipole tilt effect, the lobe reconnection between the summer and winter hemispheres have different patterns, that is, magnetic field lines that drape poleward from the duskside occur only in the summer hemisphere, compared to the winter hemisphere. During the first data period, which corresponds to the northern hemisphere's summer, particular lobe reconnection signatures are easily identifiable in the simulation results. Even with a 10-min interval profile, numerous lobe reconnection signals are present in shorter time intervals, as illustrated in Figures 4a–4d.

In Figure 7a, there is no significant magnetic disturbance in the horizontal vector. However, based on the simulation results, it is evident that lobe reconnection did occur frequently in the winter hemisphere. In the summer hemisphere, the magnetic field lines drape poleward, whereas in the winter hemisphere, lobe reconnection appears quite different. As shown in Figures 7b and 9, lobe reconnection in winter does not effectively accelerate electrons to form denser FACs, so there wouldn't be significant particle precipitation, which is necessary for the formation of the expected auroral phenomenon. Additionally, we cannot neglect the role of ionospheric conductivity in this process. Any potential electric field pattern is mapped onto the ionosphere, with the exception of variations due to field-aligned potential drops. The formation of a parallel potential drop is contingent upon the convergence of ionospheric currents. The intensity of these currents, and consequently the degree of current convergence, is influenced by ionospheric conductivity. The enhanced ionospheric conductivity, resulting from solar illumination of the polar cap, enables the downward current in the cusp to connect with the upward current beyond it, thereby generating larger FACs in summer than in winter (Frey, 2007; Lyons, 1981). The seasonal dependence observed in the 15MLT-PCA is likely due to a combination of several factors.

Notably, the simulation results indicated that particular continuous lobe reconnection signatures appeared several dozen minutes before the 15MLT-PCA was observed. Feng et al. (2021) reported that the occurrence of 15MLT-PCA requires tens of minutes of steady positive IMF B_y, which may represent the process of solar wind magnetic energy flux accumulating in the tail lobe. The accumulation of magnetic flux energy influenced by the dipole tilt may be a necessary condition for the magnetic field lines draping poleward. During the data period corresponding to winter, although lobe reconnection occurs frequently, it becomes very difficult to identify the magnetic field lines that drape poleward in the simulation results. In the winter hemisphere, the magnetic flux energy cannot be effectively accumulated, resulting in the failure of the magnetic field lines to drape poleward.

Based on this understanding, we believe that the dipole tilt effect, which causes the particular pattern of lobe reconnection to occur only in the summer hemisphere, is the underlying physical mechanism for the seasonal dependence of the 15MLT-PCA.

6. Conclusions

To address the controversy over which potential explanation is more reasonable for the seasonal dependence of 15MLT-PCA in observations, we examined two data periods, both with stable positive IMF B_y observed by

DMSP/SSUSI. This investigation involved a combination of observations and simulations. Our main conclusions regarding the seasonal dependence of 15MLT-PCA can be summarized as follows:

1. The occurrence of 15MLT-PCA shows a significant seasonal dependence. During periods dominated by positive IMF B_y, 15MLT-PCA can be observed in the summer hemisphere, while no similar auroral structure appears in the winter hemisphere.
2. Lobe reconnection occurs frequently in both the winter and summer hemispheres. However, the pattern of lobe reconnection differs between the summer and winter hemispheres. The magnetic field lines that drape poleward in the winter hemisphere appear to be much rarer compared to those in the summer hemisphere.
3. We suggest that the particular pattern of lobe reconnection during the summer plays a role in the seasonal dependence of 15MLT-PCA.

Due to the dipole tilt effect, there is a significant difference in lobe reconnection between the winter and summer hemispheres. The large tilt angle in summer causes the magnetic field lines to drape poleward, contributing to the exclusive occurrence of the 15MLT-PCA during the summer. Combined evidence from both observations and simulations supports this hypothesis. Undeniably, the intensity of ionospheric currents, and consequently the strength of current density convergence, is influenced by ionospheric conductivity. Therefore, ionospheric conductivity can affect the generation process of the 15MLT-PCA. The seasonal dependence of the 15MLT-PCA appears to result from a combination of several factors. Lobe reconnection occurring in the summer hemisphere provides the primary driving force. The high ionospheric conductivity, resulting from solar illumination of the polar cap, then enables the downward current in the cusp to connect with the upward current poleward of it, driving larger FACs in summer than in winter. Nonetheless, there remain unresolved issues that necessitate further investigation.

Data Availability Statement

We would like to thank Johns Hopkins University Applied Physics Laboratory for providing the DMSP/SSUSI auroral FUV data (https://ssusi.jhuapl.edu/data_products). We acknowledge the use of NASA/GSFC's Space Physics Data Facility's OMNIWeb service at https://cdaweb.gsfc.nasa.gov/index.html/. We thank the AMPERE team and the AMPERE Science Data Center for providing data products derived from the Iridium Communications constellation, enabled by support from the National Science Foundation. Instructions for obtaining these data can be found at http://ampere.jhuapl.edu/. We acknowledge the Community Coordinated Modeling Center (CCMC) for providing the Open Geospace General Circulation Model (Open GGCM) (https://ccmc.gsfc.nasa.gov/models/).

Acknowledgments
This work was supported by the National Natural Science Foundation of China (42030101 and 42374191).

References

Akasofu, S.-I. (1964). The development of the auroral substorm. *Planetary and Space Science*, *12*(4), 273–282. https://doi.org/10.1016/0032-0633(64)90151-5

Akasofu, S.-I. (1980). The solar wind-magnetosphere energy coupling and magnetospheric disturbances. *Planetary and Space Science*, *28*(5), 495–509. https://doi.org/10.1016/0032-0633(80)90031-8

Berkey, F. T., Cogger, L. L., Ismail, S., & Kamide, Y. (1976). Evidence for a correlation between sun-aligned arcs and the interplanetary magnetic field direction. *Geophysical Research Letters*, *3*(3), 145–147. https://doi.org/10.1029/GL003i003p00145

Burch, J. L., Reiff, P. H., Menietti, J. D., Heelis, R. A., Hanson, W. B., Shawhan, S. D., et al. (1985). IMF B_y dependent plasma flow and Birkeland currents in the dayside magnetosphere: 1. Dynamics explorer observations. *Journal of Geophysical Research*, *90*(A2), 1577–1593. https://doi.org/10.1029/ja090ia02p01577

Cai, L., Kullen, A., Zhang, Y., Karlsson, T., & Vaivads, A. (2021). DMSP Observations of high-latitude dayside aurora (HiLDA). *Journal of Geophysical Research: Space Physics*, *126*(4), e2020JA028808. https://doi.org/10.1029/2020ja028808

Carter, J. A., Milan, S. E., Fogg, A. R., Paxton, L. J., & Anderson, B. J. (2018). The association of high-latitude dayside aurora with NBZ field-aligned currents. *Journal of Geophysical Research: Space Physics*, *123*(5), 3637–3645. https://doi.org/10.1029/2017ja025082

Crooker, N. U. (1979). Dayside merging and cusp geometry. *Journal of Geophysical Research*, *84*(A3), 951–959. https://doi.org/10.1029/ja084ia03p00951

Dungey, J. W. (1961). Interplanetary magnetic fields and the auroral zones. *Physical Review Letters*, *6*(2), 47–48. https://doi.org/10.1103/physrevlett.6.47

Elphinstone, R. D., Hearn, D., Murphree, J. S., & Cogger, L. L. (1991). Mapping using the tsyganenko long magnetospheric model and its relationship to viking auroral images. *Journal of Geophysical Research*, *96*(A2), 1467–1480. https://doi.org/10.1029/90ja01625

Fear, R. C., & Milan, S. E. (2012a). Ionospheric flows relating to transpolar arc formation. *Journal of Geophysical Research*, *117*(A9), A09230. https://doi.org/10.1029/2012ja017830

Fear, R. C., & Milan, S. E. (2012b). The IMF dependence of the local time of transpolar arcs: Implications for formation mechanism. *Journal of Geophysical Research*, *117*(A3), A03213. https://doi.org/10.1029/2011JA017209

Feng, H. T., Han, D. S., Qiu, H. X., Shi, R., Yang, H. G., & Zhang, Y. L. (2021). Observational properties of 15MLT-PCA in the Southern Hemisphere and the switching effects of IMF B_y on 15MLT-PCA occurrence. *Journal of Geophysical Research: Space Physics*, *126*(12), e2021JA029140. https://doi.org/10.1029/2021ja029140

Frey, H. U. (2007). Localized aurora beyond the auroral oval. *Reviews of Geophysics*, *45*(1), RG1003. https://doi.org/10.1029/2005rg000174

Frey, H. U., Han, D., Kataoka, R., Lessard, M. R., Milan, S. E., Nishimura, Y., et al. (2019). Dayside aurora. *Space Science Reviews*, *215*(8), 51. https://doi.org/10.1007/s11214-019-0617-7

Frey, H. U., Immel, T. J., Lu, G., Bonnell, J., Fuselier, S. A., Mende, S. B., et al. (2003). Properties of localized, high latitude, dayside aurora. *Journal of Geophysical Research*, *108*(A4), 8008. https://doi.org/10.1029/2002JA009332

Frey, H. U., Østgaard, N., Immel, T. J., Korth, H., & Mende, S. B. (2004). Seasonal dependence of localized, high-latitude dayside aurora (HiLDA). *Journal of Geophysical Research*, *109*(A4), A04303. https://doi.org/10.1029/2003JA010293

Fuselier, S. A., Frey, H. U., Trattner, K. J., Mende, S. B., & Burch, J. L. (2002). Cusp aurora dependence on interplanetary magnetic field B_z. *Journal of Geophysical Research*, *107*(A7), SIA6-1–SIA6-10. https://doi.org/10.1029/2001JA90065

Gou, X. C., Shi, Q. Q., Tian, A. M., Sun, W. J., Dunlop, M. W., Fu, S. Y., et al. (2016). Solar wind plasma entry observed by cluster in the high-latitude magnetospheric lobes. *Journal of Geophysical Research: Space Physics*, *121*(5), 4135–4144. https://doi.org/10.1002/2015JA021578

Han, D., Xiong, Y., Shi, R., Qiu, H., & Feng, H. (2023). A unified model of Cusp spot, High Latitude Dayside aurora (HiLDA)/(Space Hurricane), and 15MLT-PCA. *Earth and Planetary Physics*, *7*(4), 513–519. https://doi.org/10.26464/epp2023046

Han, D. S., Feng, H. T., Zhang, H., Zhou, S., & Zhang, Y. (2020). A new type of polar cap arc observed in the ~1500 MLT sector: 1. Northern Hemisphere observations. *Geophysical Research Letters*, *47*(20), e2020GL090261. https://doi.org/10.1029/2020gl090261

Hosokawa, K., Kullen, A., Milan, S., Reidy, J., Zou, Y., Frey, H. U., et al. (2020). Aurora in the polar cap: A review. *Space Science Reviews*, *216*(1), 15. https://doi.org/10.1007/s11214-020-06373

Iijima, T., & Potemra, T. A. (1976). The amplitude distribution of field-aligned currents at Northern high latitudes observed by Triad. *Journal of Geophysical Research*, *81*(13), 2165–2174. https://doi.org/10.1029/JA081i013p02165

Korth, H., Anderson, B. J., Zurbuchen, T. H., Slavin, J. A., Perri, S., Boardsen, S. A., et al. (2010). The interplanetary magneticfieldenvironment at Mercury's orbit. *Planetary and Space Science*, *59*(15), 2075–2085. https://doi.org/10.1016/j.pss.2010.10.014

Kullen, A. (2012). Transpolar arcs: Summary and recent results. In *Auroral phenomenology and magnetospheric processes: Earth and other planets* (pp. 69–80). https://doi.org/10.1029/2011GM001183

Kullen, A., Brittnacher, M., Cumnock, J. A., & Blomberg, L. G. (2002). Solar wind dependence of the occurrence and motion of polar auroral arcs: A statistical study. *Journal of Geophysical Research*, *107*(A11), 13-1–13-23. https://doi.org/10.1029/2002ja009245

Le, G., Lu, G., Strangeway, R. J., & Pfaff, R. F. (2002). Strong interplanetary magnetic field B_y-related plasma convection in the ionosphere and cusp field-aligned currents under northward interplanetary magnetic field conditions. *Journal of Geophysical Research*, *107*(A12), 1477. https://doi.org/10.1029/2001JA007546

Liou, K., & Mitchell, E. (2019). Effects of the interplanetary magnetic field y component on the dayside aurora. *Geoscience Letters*, *6*(1), 11. https://doi.org/10.1186/s40562-019-0141-3

Luhmann, J. R., Walker, R. J., Russell, C. T., Crooker, N. U., Spreiter, J. R., & Stahara, S. S. (1984). Patterns of potential magnetic field merging sites on the dayside magnetopause. *Journal of Geophysical Research*, *89*(A3), 1739–1742. https://doi.org/10.1029/ja089ia03p01739

Lyons, L. R. (1981). The field-aligned current versus electric potential relation and auroral electrodynamics, Physics of Auroral Arc Formation. In J. R. Kan & S.-I. Akasofu (Eds.), *Geophysical monograph 25* (p. 252). American Geophysical Union.

Milan, S. E., & Grocott, A. (2021). High latitude ionospheric convection. In *In ionosphere dynamics and applications* (pp. 21–47).

Milan, S. E., Lester, M., Cowley, S. W. H., & Brittnacher, M. (2000). Dayside convection and auroral morphology during an interval of northward interplanetary magnetic field. *Annals of Geophysics*, *18*(4), 436–444. https://doi.org/10.1007/s005850050901

Murphree, J. S., Cogger, L. L., & Anger, C. D. (1981). Characteristics of the instantaneous auroral oval in the 1200–1800 MLT sector. *Journal of Geophysical Research*, *86*(A9), 7657–7668. https://doi.org/10.1029/JA086iA09p07657

Newell, P. T. (2000). Reconsidering the inverted-V particle signature: Relative frequency of large-scale electron acceleration events. *Journal of Geophysical Research*, *105*(A7), 15779–15794. https://doi.org/10.1029/1999JA000051

Newell, P. T., Burke, W. J., Meng, C.-I., Sanchez, E. R., & Greenspan, M. E. (1991). Identification and observations of the plasma mantle at low altitude. *Journal of Geophysical Research*, *96*(A1), 35–45. https://doi.org/10.1029/90JA01760

Østgaard, N., Mende, S. B., Frey, H. U., & Sigwarth, J. B. (2005). Simultaneous imaging of the reconnection spot in the opposite hemispheres during northward IMF. *Geophysical Research Letters*, *32*(21), L21104. https://doi.org/10.1029/2005GL024491

Østgaard, N., Reistad, J. P., Tenfjord, P., Laundal, K. M., Rexer, T., Haaland, S. E., et al. (2018). The asymmetric geospace as displayed during the geomagnetic storm on 17 August 2001. *Annales Geophysicae*, *36*(6), 1577–1596. https://doi.org/10.5194/angeo-36-1577-2018

Papitashvili, V. O., Belov, B. A., Faermark, D. S., Feldstein, Y. I., Golyshev, S. A., & Levitin, A. E. (1994). Electric potential patterns in the northern and southern polar regions parameterized by the interplanetary magnetic field. *Journal of Geophysical Research*, *99*(A7), 13251–13262. https://doi.org/10.1029/94ja00822

Paxton, L. J., Meng, C.-I., Fountain, G. H., Ogorzalek, B. S., Darlington, E. H., Goldsten, J., & Peacock, K. (1992). SSUSI: Horizon-Tohorizon and limb-viewing spectrographic imager for remote sensing of environmental parameters, Ultraviolet Technology IV. *SPIE*, *1764*, 161–176.

Raeder, J. (2003). Global geospace modeling: Tutorial and review. In *Space plasma simulation* (Vol. 615, p. 84). Springer.

Raeder, J., Larson, D., Li, W., Kepko, E. L., & Fuller-Rowell, T. (2008). OpenGGCM simulations for the THEMIS mission. *Space Science Reviews*, *141*(1–4), 535–555. https://doi.org/10.1007/s11214-008-9421-5

Reiff, P. H., & Burch, J. L. (1985). B_y-dependent dayside plasma flow and Birkeland currents in the dayside magnetosphere, 2, a global model for northward and southward IMF. *Journal of Geophysical Research*, *90*(A2), 1595–1609. https://doi.org/10.1029/ja090ia02p01595

Reistad, J. P., Laundal, K. M., Østgaard, N., Ohma, A., Burrell, A. G., Hatch, S. M., et al. (2021). Quantifying the lobe reconnection rate during dominant IMF B_y periods and different dipole tilt orientations. *Journal of Geophysical Research: Space Physics*, *126*(11), e2021JA029742. https://doi.org/10.1029/2021ja029742

Ruohoniemi, J. M., & Greenwald, R. A. (1996). Statistical patterns of high latitude convection obtained from Goose Bay HF radar observations. *Journal of Geophysical Research*, *101*(A10), 21743–21763. https://doi.org/10.1029/96JA01584

Sato, T., & Iijima, T. (1979). Primary sources of large scale Birkeland currents. *Space Science Reviews*, *24*(3), 347–366. https://doi.org/10.1007/BF00212423

Trattner, K. J., Petrinec, S. M., & Fuselier, S. A. (2021). The location of magnetic reconnection at Earth's magnetopause. *Space Science Reviews*, *217*(3), 41. https://doi.org/10.1007/s11214-021-00817-8

Weimer, D. R. (2001). Maps of ionospheric field-aligned currents as a function of the interplanetary magnetic field derived from Dynamics Explorer 2 data. *Journal of Geophysical Research*, *106*(A7), 12889–12902. https://doi.org/10.1029/2000JA000295

Zhang, Q. H., Zhang, Y. L., Wang, C., Oksavik, K., Lyons, L. R., Lockwood, M., et al. (2021). A space hurricane over the Earth's polar ionosphere. *Nature Communications*, *12*(1), 1207. https://doi.org/10.1038/s41467-021-21459-y

Zhu, C. B., Zhang, H., Ge, Y. S., Pu, Z. Y., Liu, W. L., Wan, W. X., et al. (2015). Dipole tilt angle effect on magnetic reconnection locations on the magnetopause. *Journal of Geophysical Research: Space Physics*, *120*(7), 5344–5354. https://doi.org/10.1002/2015JA020989